Hydrogen-Bond Disruption by Vibrational Excitations in Water

ARTICLE *in* THE JOURNAL OF PHYSICAL CHEMISTRY A · JUNE 2007

Impact Factor: 2.69 · DOI: 10.1021/jp069027g · Source: PubMed

3 AUTHORS:

Zhaohui Wang
Xiamen University
34 PUBLICATIONS **1,065** CITATIONS
SEE PROFILE

Yoonsoo Pang
Gwangju Institute of Science and Technology
28 PUBLICATIONS **526** CITATIONS
SEE PROFILE

Dana D Dlott
University of Illinois, Urbana-Champaign
297 PUBLICATIONS **6,631** CITATIONS
SEE PROFILE

FEATURE ARTICLE

Hydrogen-Bond Disruption by Vibrational Excitations in Water

Zhaohui Wang, Yoonsoo Pang, and Dana D. Dlott*

School of Chemical Sciences, University of Illinois at Urbana-Champaign, 600 South Mathews Avenue, Urbana, Illinois 61801

Received: December 29, 2006; In Final Form: February 12, 2007

An excitation of the OH-stretch ν_{OH} of water has unique disruptive effects on the local hydrogen bonding. The disruption is not an immediate vibrational predissociation, which is frequently the case with hydrogen-bonded clusters, but instead is a delayed disruption caused by a burst of energy from a vibrationally excited water molecule. The disruptive effects are the result of a fragile hydrogen-bonding network subjected to a large amount of vibrational energy released in a short time by the relaxation of ν_{OH} stretching and δ_{H_2O} bending excitations. The energy of a single ν_{OH} vibration distributed over one, two, or three (classical) water molecules would be enough to raise the local temperature to 1100, 700, or 570 K, respectively. Our understanding of the properties of the metastable water state having this excess energy in nearby hydrogen bonds, termed H_2O^*, has emerged as a result of experiments where a femtosecond IR pulse is used to pump ν_{OH}, which is probed by either Raman or IR spectroscopy. These experiments show that the H_2O^* spectrum is blue-shifted and narrowed, and the spectrum looks very much like supercritical water at ∼600 K, which is consistent with the temperature estimates above. The H_2O^* is created within ∼400 fs after ν_{OH} excitation, and it relaxes with an 0.8 ps lifetime by re-formation of the disrupted hydrogen-bond network. Vibrationally excited H_2O^* with one quantum of excitation in the stretching mode has the same 0.8 ps lifetime, suggesting it also relaxes by hydrogen-bond re-formation.

1. Introduction

Water is an exceedingly complicated liquid, so it should come as no surprise that vibrational excitations of water exhibit complex and unusual properties. Vibrational excitations of water are so complicated, in part, because water has just enough atoms to be a polyatomic molecule, water has more hydrogen bonds (3.59 on average) than atoms (3), the hydrogen bonds are fragile, they exist only fleetingly, and they are continually broken and re-formed on the picosecond time scale.[1−3] The energy of a vibrational excitation in water is quite sufficient, under the right circumstances, to create a sizable transient disruption of the local hydrogen bonding. Staib and Hynes[4] proposed that excitation to $\upsilon = 1$ of the OH-stretch ν_{OH} (3000−3700 cm^{-1}) might result in a prompt vibrational predissociation process that breaks a hydrogen bond. Although such predissociation processes are facile in isolated water clusters,[5] no evidence for them has been found in liquid water.[6] However, there is now abundant evidence that ν_{OH} excitation disrupts water's hydrogen bonding by a delayed process resulting from the energy burst created by vibrational relaxation (VR). The idea of vibrational excitation of a hydrogen-bonded liquid leading to hydrogen bond breaking is not new. The heating in water associated with IR pump pulses obviously leads to a time-delayed weakening or breaking of hydrogen bonds in the equilibrated liquid,[7] but we mean specifically the nonequilibrium cleavege of hydrogen bonds. The first direct observation of a delayed nonequilibrium cleavage of hydrogen bonds should be attributed, we believe, to the Fayer group, who studied OD stretches of alcohol oligomers in CCl_4,[8−10] and OD-stretch excitations of HOD in H_2O.[11]

Much of what we know about vibrational excitations in water has been discovered in the past few years as a result of pump−probe experiments using ultrashort IR pulses. The ν_{OH} and water bending excitations δ_{H_2O} each have vibrational relaxation (VR) lifetimes of about 0.2 ps,[7,12−14] so about 0.4 ps after ν_{OH} excitation a sizable amount of energy is pumped into local bath modes such as water torsions and hydrogen bond stretches. This metastable state of water—no stretching or bending excitations but a great deal of energy in the adjacent hydrogen bonds—will henceforth be termed H_2O^*. As we shall show below, there is no single H_2O^* state but rather an inhomogeneous distribution of configurations with weakened hydrogen bonding. Unless we specifically indicate $\upsilon = 1$, H_2O^* will refer to molecules with ν_{OH} in the $\upsilon = 0$ vibrational ground state. The H_2O^* species decays into a thermalized state[15,16] characterized by a temperature jump ΔT. Measurements of the H_2O^* lifetime range from 0.6 to 0.8 ps.[7,12−16] The behavior of ν_{OH} excitations in water is depicted schematically in Figure 1. When IR photons excite ν_{OH} to the $\upsilon = 1$ state, VR causes each excited molecule to emit a burst of mechanical energy. Eventually, these energy bursts thermalize in time and space, resulting in an equilibrium temperature jump ΔT. The energy bursts are intense. Here is a crude but effective way of understanding the H_2O^* state. If 3400 cm^{-1} of energy were added to a classical nonlinear triatomic molecule ($C_v = 6k_B$), the local temperature would be 1100 K (Figure 1a). If this energy were spread out over two or three

* Corresponding author. E-mail dlott@scs.uiuc.edu.

10.1021/jp069027g CCC: $37.00
Published on Web 03/22/2007

Dana D. Dlott was born in Los Angeles, CA, in 1952, and he lived in Dayton, OH, and Indianapolis, IN, before attending college at Columbia University. He received an A.B. degree from Columbia in 1974 and a Ph.D. in chemistry from Stanford University in 1979 under Prof. M. D. Fayer. He subsequently joined the faculty at the University of Illinois at Urbana-Champaign. Dlott is a Fellow of APS, OSA, and AAAS, and his research interests are in the areas of condensed phase molecular dynamics and dynamics of molecular materials.

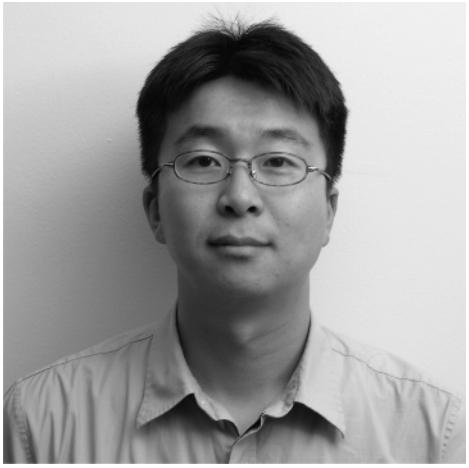

Yoonsoo Pang received a Bachelor's and a Master's degree in chemistry from Seoul National University, Korea, in 1996 and 1998, respectively. After spending three years as a lecturer at Korea Military Academy, he joined a Ph.D. program at University of Illinois at Urbana-Champaign under the supervision of Prof. Dana D. Dlott. His thesis research is focused on vibrational energy transfer in molecular nanostructures and vibrational energy relaxation of water.

molecules (Figure 1b,c), the local temperatures would be 700 or 570 K, respectively. Obviously, we could get different answers using other models for the local heat capacity, for instance to include the hydrogen bonding, but the picture of high local temperatures would be unchanged.

It takes only elementary thermodynamics to understand the equilibrium properties of water post thermalization (Figure 1d). Because picosecond time scale heating is isochoric, ΔT is associated with a pressure jump ΔP. (For small values of ΔT in water, $\Delta P = \Delta T \times 18$ atm).[17] The values of either ΔT or ΔP (they are not independent) are determined by bulk parameters such as the laser pulse intensity; in works cited here ΔT ranges from quite small[7,12,14,18] ($\Delta T \approx 2$ K) to moderate ($\Delta T \approx 30$ K)[6,15,16,19,20] to large enough ($\Delta T > 100$ K) to cause laser ablation via a phase explosion.[17] In contrast, the size of the energy burst emitted by the excited water molecules depends solely on the energy $h\nu$ of the IR photons; this energy is largely outside the control of the experimenter who can vary the size of each burst by only ~20%, by tuning the IR pulse from 3000

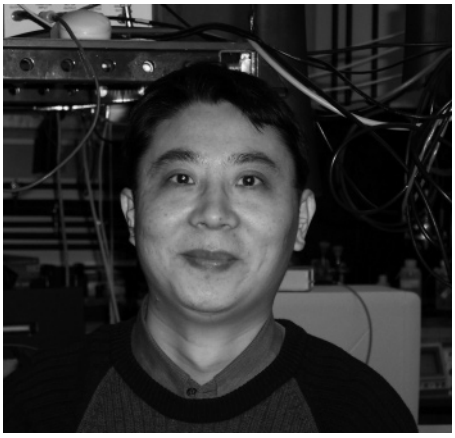

Zhaohui Wang received a B.S. degree in chemistry and an M.S. in physical chemistry from Fudan University at 1991 and 1994, respectively, and a Ph.D. degree in physical chemistry from the Institute of Chemistry, Chinese Academy of Sciences, in 1997. He worked as a postdoctoral research associate from 1998 to 2000 under the supervision of Prof. Sanford Ruhman at Hebrew University. Currently he is working in the laboratory of Prof. Dana D. Dlott as a research associate. His research interests are in the areas of femtosecond vibrational spectroscopy, vibrational dynamics in condensed phases, and energy transport at surfaces and interfaces.

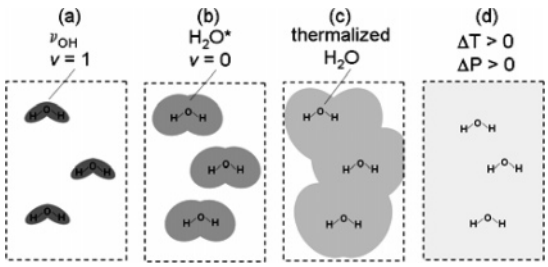

Figure 1. Transient disruption of hydrogen bonding by vibrationally excited water. (a) Water molecules with excited OH-stretch, ν_{OH}. (b) Vibrational relaxation of ν_{OH} generates an energy burst from each excited molecule that disrupts the local hydrogen bonding to create H_2O^* in the vibrational ground state. (c), (d) The H_2O^* thermalizes and the excess energy becomes uniformly distributed in time and space to produce an equilibrium state with a temperature jump ΔT and a pressure jump ΔP.

to 3700 cm^{-1}. *No matter how large or small the IR pulse intensity or the value of* ΔT*, the size of the energy burst in water remains approximately constant.*

Most studies of vibrational energy in water use the IR pump−probe method, but in our lab we have used an IR pump combined with a Raman probe. The data we acquired over the past several years[20] show several effects—spectra with two distinct components, long-lived states, and so on—that have not been seen in IR experiments performed in other labs.[21] The Bakker group has proposed an explanation for this conundrum.[21,22] They note that our 0.8 ps pump pulses are quite a bit longer in duration than the 0.1−0.3 ps pulses used by these other groups, and in fact are longer than the 0.2 ps time constants for either ν_{OH} or δ_{H_2O} relaxation or the ~0.4 ps time constant for H_2O^* formation. So in our experiments we can create H_2O^* with the leading edge of the pump pulses, and then re-excite it to the H_2O^* $v = 1$ state with the trailing edge of the pulse.[21,22] Furthermore, because H_2O^* is the longest-lived species in the thermalization of ν_{OH}, with longer-duration pump pulses, it tends to accumulate to a greater extent than either ν_{OH} or δ_{H_2O} species. Bakker's proposal is a good start toward explaining many differences seen in the IR and Raman measurements. Because of the sensitivity of our Raman measurements to H_2O^*, our

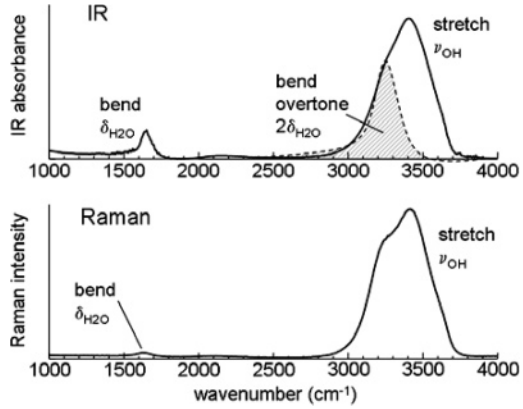

Figure 2. IR and Raman spectra of water, showing the OH-stretching (ν_{OH}) region and bending (δ_{H_2O}) region. The shaded region indicates the approximate location of the bend overtone $2\delta_{H_2O}$. Reproduced from ref 20.

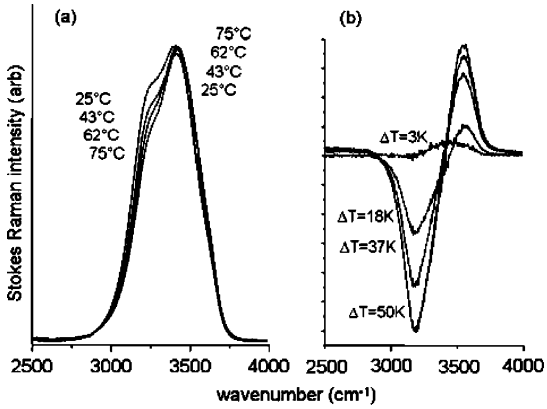

Figure 3. (a) Raman spectra of water at the indicated temperatures. Heating water at constant pressure reduces the density and decreases the overall strength of hydrogen bonding. (b) Difference spectra with the ambient temperature spectrum subtracted away.

measurements contain new information about the ground and excited states of H_2O^*, its lifetime and its VR pathways.

This Feature Article will focus on vibrational energy in water. Two closely related areas in which there is a great deal of activity, vibrational coherence studies of hydrogen bond fluctuations in water and vibrational energy in HOD present as a dilute solute in either D_2O or H_2O (HOD/D_2O or HOD/H_2O), will be discussed only to the extent needed to understand the water results.

In the rest of this paper we provide a brief discussion of water vibrational spectroscopy and a brief historical review of ultrafast IR studies that focuses on water, with just a brief mention of the extensive literature on HOD/D_2O. Then we describe experiments performed in our laboratory and others to create and characterize the H_2O^* state of water created from ν_{OH} excitation.

2. Vibrational Spectroscopy of Water

Figure 2 shows the IR and Raman spectra of water.[19] The isolated H_2O molecule with C_{2v} symmetry has three vibrations, the two stretching vibrations ν^s_{OH} and ν^a_{OH} and the bending vibration δ_{H_2O}.[23] In the gas phase ν^s_{OH} and ν^a_{OH} are located at 3652 and 3755 cm^{-1}.[23] Liquid water is an extensively hydrogen-bonded environment. In this generally locally asymmetric liquid environment, it is better to think of the stretching vibrations ν_{OH} as local excitations of the OH atomic groups[24] whose frequencies are fluctuating on the picosecond time scale in response to time variations in hydrogen bonding.[1,25−27] Liquid-state hydrogen bonding results in an immense broadening and red-shifting of the ν_{OH} transition.[25,26,28−30] The effects of hydrogen bonding on δ_{H_2O} are less dramatic. The asymmetric shape of the ∼100 cm^{-1} fwhm transition δ_{H_2O} results from a superposition of water molecules with varying states of hydrogen bonding.[31,32] The water libron is not shown in Figure 2; it is centered near 700 cm^{-1} with a fwhm of ∼300 cm^{-1}.[31,32] The combination band of the bend and libron is seen in the 2000−2500 cm^{-1} range of Figure 2. Hydrogen bond stretching excitations also not shown in Figure 2 are located in the <200 cm^{-1} spectral region.

In Figure 2 we have illustrated[19] a "bend overtone" region, which was computed using the observed bend spectrum and the gas-phase anharmonic red shift.[23] This figure suggests a Fermi resonance in liquid water (i.e., a 2:1 resonance between stretch and bend overtone) that does not exist in the gas phase and also suggests that the greatest coupling between stretch and bend occurs in water molecules that instantaneously possess a larger red shift due to a stronger hydrogen-bonding environment.

One of the most intellectually compelling features of ultrafast vibrational studies of water dynamics[28,30,33] stems from the unique relationship between the ν_{OH} frequency and the length and strength of the hydrogen bonds. The greater the frequency red shift away from the ∼3700 cm^{-1} frequency of the free water transition, the stronger the hydrogen bond. Specifically, we mean for the OH group being observed, the donor hydrogen bond typically expressed as O−H···O. Bratos[33] introduced the idea that a water pump−probe experiment could make it possible to watch hydrogen bonds stretch, contract, break, and re-form in real time, at least to the extent that frequency red shift and hydrogen bond *strength* was correlated with hydrogen bond *length*. In recent years there has been a great deal of activity in the theory of pump−probe and vibrational coherence measurements of water and HOD.[25,26,28−30,34−43]

The idea of an approximately linear correlation between the hydrogen bond length and the frequency red shift is an old one.[44] Originally, the correlation was developed by looking at the O···O distances of water in solid inorganic hydrates whose structures were known from X-ray diffraction, and this correlation was frequently applied even in aqueous environments. The Skinner group[30] and the Hynes group[28] both tested the idea of a length−red-shift correlation in liquid water using molecular simulations. During an MD trajectory, a tagged water molecule experienced different hydrogen bonding states and its instantaneous ν_{OH} frequencies fluctuated. Both groups reported similar findings. There was a reasonably good correlation between length and red shift, but at a given ν_{OH} frequency there was actually a range of hydrogen bond lengths (alternatively a particular length represents a range of ν_{OH} frequencies), with the dispersion due to the spread of hydrogen-bonding angles and variations in the states of the acceptor hydrogen bonding.

Increasing the temperature weakens hydrogen bonding in water. Figure 3 illustrates the temperature dependence of the ν_{OH} transition of water. This transition makes a reasonably good thermometer. In equilibrium, at ambient temperature the average number of HB in water is 3.59. With $\Delta T = 75$ K (i.e., at the boiling point, 100 °C) this average decreases to 3.24.[45] As temperature is increased, the red part of the ν_{OH} transition loses intensity and the blue part gains intensity.[11] The difference spectrum shown in Figure 3b exhibits a characteristic derivative shape that we shall see frequently in our data.

The Fayer group has provided a spirited argument to the effect that data such as that shown in our Figure 3 and Figure 2 of ref

11 should not be interpreted as arising from hydrogen bond weakening, but rather as arising from a temperature-dependent change in the concentration of water molecules with a broken hydrogen bond. They[11] argue that overall weakening would result in a continuous blue shift with increasing temperature, whereas the actual spectra seem to consist of two components with varying amplitudes that shift very little. Although this is an attractive hypothesis and may very well be correct, we urge caution. Historical evidence has shown that vibrational spectroscopy has not been a reliable method for determining water structures. In addition, at liquid densities where there is a broad range of hydrogen-bonding parameters, it requires a certain arbitrary distinction to determine whether a hydrogen bond is "present" or "broken".

3. IR−IR and IR−Raman Measurements

3.1. IR Pumping. A technical issue that arises in water measurements results from the large IR absorption coefficient α in the ν_{OH} region.[46] The (1/e) absorption depth α^{-1} is less than 1 μm at the water absorption peak, requiring an inconveniently thin sample cell, especially if the water sample is to be flowed across the IR laser beam for thermal management. This difficulty is in part the motivation behind the more numerous studies of HOD/D_2O, where by dilution α can be tuned by the experimenter. (The other motivation is the attraction of studying a molecule, HOD, with just one rather than two OH or OD stretching excitations.) Nevertheless, researchers have found novel solutions such as nanofabricated cuvettes[18] or tuning the pump pulses to the extreme edge of the absorption spectrum.[47]

An IR pump pulse heats the sample volume nonuniformly. Femtosecond IR pulses usually have a nominal Gaussian radial intensity distribution. IR absorption causes the pulse intensity to be attenuated exponentially with increasing distance below the irradiated surface. The hottest region of the sample is located at the irradiated surface, at the center of the IR beam. The temperature jump at the hottest point will be denoted ΔT. Because picosecond time scale heating is adiabatic and isochoric, a spatially nonuniform temperature jump creates a similar nonuniform pressure jump ΔP.[17] The pressure jump ΔP relaxes much faster than the temperature jump ΔT. The internal pressure causes a rapid volume expansion, primarily along the direction perpendicular to the irradiated surface.[17] For a pumped volume $\sim$1 μm thick and an expansion at about the speed of sound ($\sim$1 km/s or 1 μm/ns), ΔP should relax in about 1 ns. The temperature jump ΔT relaxes by thermal conduction into the part of the liquid not pumped by IR, or into the windows of the sample cell. This cooling process typically occurs on the 100 μs time scale, far slower than the picosecond time scale measurements but faster than the 1 ms interval between laser pulses. For extra care in eliminating heating effects, many researchers (including us) flow the water to refresh the sample between pulses.

With a Gaussian profile IR pulse of energy E_p, the *average* fluence $J_{avg} = E_p/(\pi r_0^2)$, but the *peak* fluence at the beam center is *twice this value*, $J_c = 2E_p/(\pi r_0^2)$. The peak energy density E_v in the water is given by $E_v = J_c\alpha$. Values of α for pure water are tabulated in ref 46. The peak temperature and pressure jumps are[48]

$$\Delta T = \frac{J_c\alpha}{\rho C_v} = \frac{2E_p\alpha}{\pi {r_0}^2 \rho C_v} \quad (1)$$

and

$$\Delta P \approx (\partial P/\partial T)_V \Delta T = (\beta/\kappa_T)\Delta T \quad (2)$$

where β is the coefficient of thermal expansion and κ_T is the isothermal compressibility. For ambient water, $\rho C_v = 4.2$ MJ K^{-1} m^{-3} and $(\partial P/\partial T)_V = 1.8$ MPa K^{-1}.

Most of the experiments reported here used $\Delta T = 30$ K, which could be accomplished, for instance, with IR pulses having $E_p = 9.5$ μJ and a Gaussian ($1/e^2$) beam radius $r_0 = 150$ μm, tuned to 3310 cm^{-1} where the absorption coefficient $\alpha = 4660$ cm^{-1}.[46] The corresponding pressure jump would be 54 MPa ($\sim$0.5 kbar). We feel that, to avoid confusion, it is important to refer to the *peak* ΔT, even though it is more usual to refer to the *average* ΔT. For water initially at 25 °C, $\Delta T = 40$ K *peak* will bring the maximum temperature of the water sample to 65 °C, but a jump of $\Delta T = 40$ K *average* will bring the water at the beam center to above the boiling point and the water will explode in a femtosecond ablation process, which seriously affects the relaxation and rate constants.[17]

3.2. Energy Levels. Figure 4a is an energy level diagram of water vibrations.[6,20] Not shown in the figure are the "bath excitations" that result from the condensed-phase environment, such as the librons and hydrogen bond stretches. The vibrational state of water is specified by $|nn'\rangle$ where n represents the stretching and n' the bending states. In the experiments being discussed here, an ultrashort IR pulse creates an initial excitation in the state $|10\rangle$. Within the ν_{OH} manifold, probe pulses can monitor three different types of transitions. *Ground-state absorption* refers to the $|00\rangle \rightarrow |10\rangle$ transition, *excited-state emission* to the $|10\rangle \rightarrow |00\rangle$ transition and *excited-state absorption* to the $|10\rangle \rightarrow |20\rangle$ transition.

3.3. Vibrational Relaxation (VR). VR pathways are usually specified in terms of the water vibrations ν_{OH} and δ_{H_2O}.[34,35,39] Thus for ν_{OH} excitations, there are two competing VR pathways[43,49] shown in Figure 4a,

$$\nu_{OH} \rightarrow \delta_{H_2O} + (\sim 1760\ cm^{-1})$$

$$\nu_{OH} \rightarrow \text{ground state} + (\sim 3400\ cm^{-1})$$

The former type of process is "stretch-to-bend" characterized by rate constant k_{SB}. A recent experimental estimate of the quantum yield for stretch-to-bend generation by Lindner et al.[13] suggests that each quantum of stretch creates almost two bending quanta, in which case the ($\sim$1760 cm^{-1}) of excess energy in the scheme above would appear mainly in the form of a second bend quantum. The latter type of process is "stretch-to-ground state" with k_{SG}. The ν_{OH} lifetime $T_1 = (k_{SB} + k_{SG})^{-1}$. For the bending vibration there is only one VR pathway,[50,51]

$$\delta_{H2O} \rightarrow \text{ground state} + (\sim 1640\ cm^{-1})$$

and the δ_{H_2O} lifetime $T_1 = (k_{BG})^{-1}$. Note that each pathway may represent a myriad of specific processes which differ in the detailed distribution of excess energy in the bath. For instance, with bend-to-ground-state relaxation, the $\sim$1640 cm^{-1} of excess energy might be distributed in a number of ways among librons and hydrogen-bond excitations.

Regardless of the detailed mechanisms of water VR, it is clear that the time constant for a water molecule to lose its vibrational energy to the surroundings, i.e., the time constant for generation of the vibrational energy burst, is $\sim$0.4 ps,[7,13] this number being an approximate time constant for decay of both the parent stretch and the daughter bend excitations.

One question that we feel needs additional investigation regards the number of intermediate states lying between

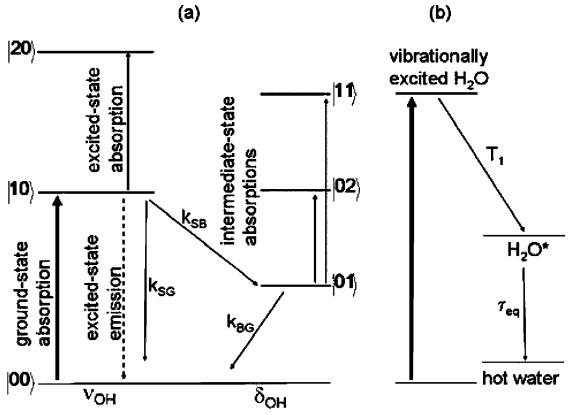

Figure 4. (a) Energy level diagram for vibrational relaxation in terms of the water vibrations ν_{OH} and δ_{H_2O}. The notation $|nn'\rangle$ means n quanta of stretch and n' quanta of bend. (b) Phenomenological model to describe ultrafast spectroscopy measurements on water. The H_2O^* state is a metastable state with a local hydrogen-bond network that is disrupted by the burst of energy created by the relaxation of ν_{OH}. T_1 is a time constant for vibrational energy loss, and τ_{eq} is a time constant for thermalization of the H_2O^* to produce a water ground state with an equilibrium temperature jump ΔT.

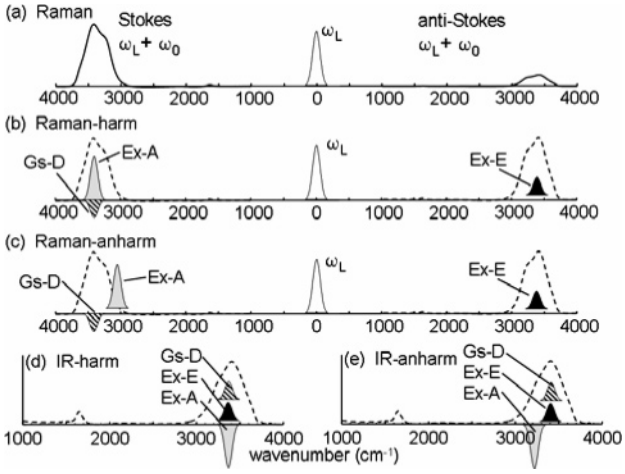

Figure 5. IR pump pulse creates an excitation in ν_{OH} that can be monitored by either a Raman or an IR probe. Both probe methods can see a depletion of the ground-state absorption (Gs-D), an excited-state emission (Ex-E) and an excited-state absorption (Ex-A). (a) With Raman spectroscopy there is a Stokes and an anti-Stokes branch; at ambient temperature the anti-Stokes signal is far weaker. (b), (c) The excited-state emission is observed in the anti-Stokes region and the excited-state absorption and ground-state depletion in the Stokes region. In the harmonic approximation (b) the excited-state absorption is partially offset by the ground-state depletion. When anharmonicity is introduced (c), the excited-state absorption is red-shifted from the ground-state depletion in the Stokes spectrum and the spectrum becomes bipolar. (d) In the IR, in the harmonic approximation, the ground-state depletion, excited-state emission, and excited-state absorption cancel, so there is no IR signal. (e) When anharmonicity is introduced, the excited-state absorption is red-shifted and a bipolar IR signal will be observed.

vibrationally excited ν_{OH} water and the final state of heated equilibrated water, or indeed, whether there are true distinguishable intermediate states or rather a complex potential energy landscape.[52] A single-intermediate model with two phenomenological time constants was originally proposed by Lock, Woutersen, and Bakker.[15,16] In this model the ν_{OH} state decayed with time constant T_1 to an intermediate state denoted 0*. The decay of ν_{OH} was indicated by the disappearance of its characteristic red-shifted excited-state absorption[21] (cf. Figures 5 and 9 below). The 0* state could in principle be probed via transitions to its excited stretching state 1*. Subsequently, 0* thermalized with time constant τ_{eq} to an equilibrium state consistent with the temperature jump ΔT. The thermalization process was indicated by the rise of a blue-shifted spectral component denoting the creation of water with weakened hydrogen bonding.[21] The spectrum of this thermalized ground state should be the same as the spectrum of water heated in a constant-volume thermostat. Measurements from the Bakker group where ν_{OH} only was probed gave $T_1 = 0.26$ ps and $\tau_{eq} = 0.55$ ps.[15,16] Because the H_2O^* state also lies along the path between ν_{OH} and the thermalized ground state, as shown in Figure 4b, it is unclear how successfully we can employ a single intermediate model such as that shown in Figure 4b or whether one or more additional intermediates such as Bakker's 0* plus H_2O^* are needed.

3.4. Raman and IR Probing. With a Raman probe, as depicted in Figure 5a, a laser pulse at ω_L is incident on the sample and the inelastically scattered light is collected, spectrally resolved, and detected with a multichannel array.[53] With no pump pulses the Stokes signal is much more intense than the anti-Stokes because $h\nu/k_BT \gg 1$ for water stretch and bend at ambient temperature. In our original experiments[19,20,54−57] we investigated only the anti-Stokes (blue-shifted) emission, but now we simultaneously monitor both Stokes (red-shifted) and anti-Stokes emission.[6] A *Raman transient* is the pump-induced change in the Raman intensity relative to a signal obtained with a probe pulse that *precedes* the pump pulse. The anti-Stokes transients have proven especially useful. Anti-Stokes signals arise from a single source, excited-state emission, and the excited states are detected against a nearly dark background.[58,59] The Stokes transients are more difficult to interpret. The Stokes transients arise from two sources, ground-state absorption depletion and excited-state absorption, and both effects are observed as small changes against a much larger background signal.[6]

In a two-color IR pump−probe experiment, the signal is the pump-induced change in the transmitted probe pulse intensity.[60] In earlier water experiments the probe pulses were detected with single-channel photodetectors,[61−66] but in more recent experiments the probe was spectrally resolved by a spectrograph and multichannel photodetector array.[7,12−14,67] Pump-induced changes in the probe intensity are small effects against a large background, but excellent signal-to-noise ratios are achievable provided the laser pulses have good intensity stability. IR probe pulse signals are more difficult to interpret than either Stokes or anti-Stokes Raman signals, because the probe pulse transmission is simultaneously sensitive to three processes, excited-state emission, ground-state absorption depletion, and excited-state absorption.[6,60]

It is useful to consider what Raman and IR experiments would see in a baseline approximation where all vibrations were harmonic, and also in the more germane framework of weakly anharmonic excitations. The diagonal anharmonicity in water is ~250 cm^{-1} (~7% of the transition frequency) for ν_{OH} and ~40 cm^{-1} for δ_{H_2O} (~2.4% of the transition frequency).[23]

With the Raman experiment in the harmonic approximation (Figure 5b), excited states created by the pump would create a sudden intensity jump in the anti-Stokes region.[6,58] In the Stokes region the combination of ground-state depletion and excited-state absorption lead to another sudden intensity jump of the same amplitude.[6] The Stokes intensity jump results from a combination of two partially offsetting factors. In the harmonic approximation the cross-section for excited-state absorption is twice that of ground-state absorption, so the ground-state depletion leads to a signal reduction whereas the excited-state

absorption leads to a signal increase that is twice as great. When anharmonicity is introduced, as depicted in Figure 5c, the anti-Stokes transients are not affected but in the Stokes spectrum the excited-state absorption becomes red-shifted away from the ground-state absorption. The Stokes transient in this case becomes bipolar, with a negative-going part from the ground-state depletion and a positive-going part of approximately twice the amplitude due to the excited-state absorption.[6] When the anharmonic shift is smaller than the vibrational line width, which is the case with water, clearly separating these two contributions to the Stokes transient becomes difficult.

With IR probing, an interesting and well-known result[59,60] is obtained in the harmonic approximation (Figure 5d). In the harmonic approximation there is no signal in an IR probe transmission measurement. The ground-state depletion increases the transmitted probe. The excited-state emission further increases the probe by the same amount. But the excited-state absorption decreases the probe enough to exactly offset the other two effects. In the anharmonic IR case (Figure 5e), the IR signal become bipolar, with a negative-going part due to excited-state absorption and a positive-going part due to the combination of ground-state depletion and excited-state emission.[61]

4. Brief History of Water VR Measurements

In the former Soviet Union in 1982, Vodopyanov and co-workers[68] studied the IR saturation of water ν_{OH} using a mode-locked solid-state laser operating at 3406 cm^{-1}, producing an ~100 ps pulse. In a 2-level system pumped in steady state, the intensity needed to saturate an optical transition $I_{sat.} = h\nu/\sigma\tau$ where σ is the absorption cross section and τ is a time constant for ground-state absorption recovery.[69] Exceedingly high intensities were needed to saturate the ν_{OH} transition, indicating that τ was much shorter than 100 ps. This time constant was estimated to be $\tau = 3$ ps. Vodopyanov found that the ν_{OH} absorption of water began to saturate when the absorbed energy density $J\alpha$ was about 1 kJ/cm^3, corresponding to a temperature rise of $\Delta T = 235$ K. The saturation effect was attributed to a massive blue shift of the absorption away from 3406 cm^{-1} caused by rapid isochoric heating accompanied by hydrogen bond breaking.[68]

In 1991 the first pump−probe measurements were made on ν_{OH} of HOD/D_2O by the Laubereau group,[61] but their 11 ps pulse duration was too long to adequately resolve the HOD VR. Beginning in 1997, several groups used two-color subpicosecond IR techniques to study ν_{OH} of HOD/D_2O; notable early contributors include the Bakker group,[64,65,70,71] the Laubereau group[62,63] and the Gale−Bratos collaboration.[33,72−74] In these measurements, the pump and probe pulses were independently tunable and narrow-band (here "narrow-band" means significantly narrower than the ~400 cm^{-1} fwhm of the ν_{OH} absorption). Although there is some variance in reported values, most recent measurements[35,70,75] give the ν_{OH} lifetime of HOD/D_2O as $T_1 = 0.9$ ps. The HOD/D_2O system has also been extensively studied by pump−probe and multidimensional coherence methods.

The first pump−probe measurements on water were performed in Bakker's group in 1999.[66] Bakker's group was studying the polarization anisotropy decay of HOD/D_2O with ~0.3 ps duration pulses, as a function of deuteration, and they obtained a data point at zero deuteration (i.e., in pure water) using a 3000 cm^{-1} probe pulse on the red edge of the ν_{OH} absorption. Shortly afterward, in 2000, the Dlott group studied water using IR−Raman, with 1.2 ps duration pulses.[19] The large absorption of water in the IR was not a problem because water is transparent to the visible (green) light used for Raman probing. Measurements by Dlott's group[19] of the ν_{OH} lifetime of HOD/D_2O were in good agreement with other groups. The ν_{OH} water lifetime was estimated at ~1 ps.

One important feature of the IR−Raman method is the ability to probe all water vibrations simultaneously, so the 2000 Dlott paper[19] was notable in that it measured both the decay of ν_{OH} excitations and the buildup and subsequent decay of δ_{H_2O}. The δ_{H_2O} bending vibrations were observed to build up with the ~1 ps ν_{OH} lifetime and subsequently decay with a lifetime in the range 0.6 ps $\leq T_1 \leq$ 1.2 ps. The quantum yield ϕ for the stretch-to-bend relaxation pathway $\nu_{OH} \rightarrow \delta_{H_2O}$ was given as $1.0 \leq \phi \leq 2.0$.[19]

In the 2002−2004 period, the Bakker group[15,16] and the Dlott group[6,20,49,54−57,76,77] continued their studies of water VR. The Bakker group used an IR probe and a very thin liquid cell and the Dlott group used Raman probing that does not require a thin cell. The picture developed by the Bakker group[21] begins with a rapid spectral diffusion process,[18] so that even though the ν_{OH} excitations were generated by a narrow-band pump pulse, they spread out in <100 fs to fill the entire ν_{OH} band shown in Figure 2. The ν_{OH} lifetime was $T_1 = 0.26$ (more recent experiments with greater time resolution[7,12,13,18] give a value closer to 0.2 ps). As discussed in section 3.3, there was a single intermediate called 0* on the pathway back to the ground state, and the decay of 0* via thermalization to heated water occurred with a time constant $\tau_{eq} = 0.55$ ps. This picture proved consistent with subsequent results obtained by the Wiersma group,[78] who used the same two-color pump−probe techniques as in the Bakker group, but who studied water in reverse micelles. When the water-to-surfactant ratio becomes large enough, the behavior of the water inside the micelle[78] approached the behavior of bulk water previously reported by Bakker.[15,16,21]

More recently, the Elsaesser group[7,12,14,18] and the Wiersma group[13] studied water using pulses that could be tuned into the stretch, bend and in Elsaesser's experiments even the libron regions. These studies provided a more comprehensive picture of events subsequent to ν_{OH} or δ_{H_2O} excitation. The thermalization process is seen to be quite complicated and the induced absorption changes associated with thermalization have a complicated wavelength dependence,[13] so fitting methods used by different groups lead to slightly different time constants. But, in general, the Wiersma and Elsaesser results agreed quite well. The VR of ν_{OH} appeared to originate from a single species, which is indicative of ultrafast spectral diffusion.[18] The ν_{OH} lifetime was given as either 0.19 ps[12] or 0.24 ps,[13] the δ_{H_2O} lifetime was given as 0.17 ps[12] or 0.26 ps,[13] and the time constant for thermalization was given as $\tau_{eq} = 0.8$ ps by both groups.[12,13] Note that this $\tau_{eq} = 0.8$ ps value appears consistent with Bakker's 0.55 ps time constant because it includes Bakker's thermalization process plus the 0.2 ps bend decay process.

Work originating in the Dlott group appeared to be inconsistent with the Bakker results[79] (and with future results that would be obtained by the Wiersma and Elsaesser groups). In work that followed the 2000 paper,[19] the pulse duration was improved from 1.2 to 0.8 ps, and 0.3 and 0.6 ps time constants were observed in anti-Stokes transients.[54] In contrast to Bakker's model, the 0.3 ps time constant was attributed to spectral diffusion and the 0.6 ps time constant was interpreted as the ν_{OH} lifetime.[20,54,56] An interesting result of the Dlott group experiments was the observation of two interconverting water species, one characterized by a broad spectrum and the other by a narrower blue-shifted spectrum.[20,54,56] The Dlott group

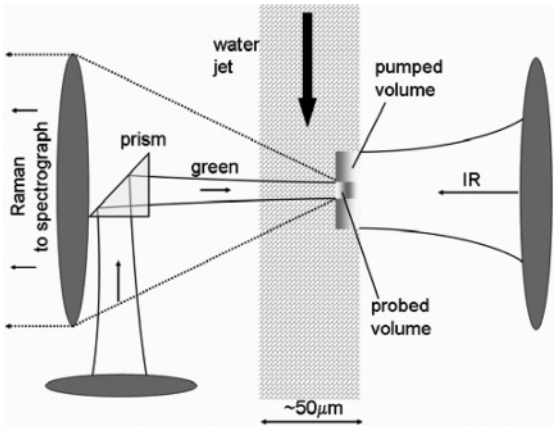

Figure 6. Optical arrangement with a water jet, and IR pump and green probe pulses. The transient Stokes and anti-Stokes Raman spectra of water are observed with a spectrograph and CCD detector. Adapted from ref 53.

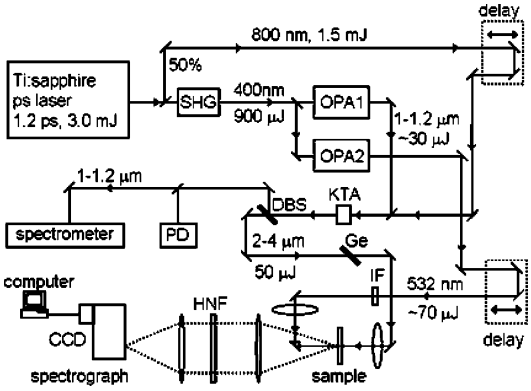

Figure 7. Block diagram of the laser system. Key: SHG = second-harmonic generator; OPA = optical parametric amplifier; KTA = potassium titanyl arsenate mixer crystal for mid-IR generation; DBS = dichroic beamsplitter; PD = photodiode; Ge = germanium filter; IF = 25 cm^{-1} fwhm interference filter at 532 nm; HNF = holographic notch filter, CCD = charge-coupled device optical detector. OPA1 is tuned from 1.0 to 1.176 μm to produce IR in the 2500−4000 cm^{-1} range, and OPA2 is fixed at 532 nm. Reproduced from ref 20.

results will be discussed in detail below in the context of Bakker's model.

5. Experimental Section

The conceptual layout of our experiment is shown in Figure 6.[53] The sample was a flowing jet of water ~50 μm thick. This jet was optically thick in the ν_{OH} absorption region. When the IR pump pulses were tuned from the peak to the edges of the ν_{OH} transition, the pulses penetrated more or less deeply into the jet, but the number of ν_{OH} excited states (equal to the number of IR photons) remained approximately constant.[53] The liquid jet was transparent to the visible Raman probe pulses.

A laser system schematic[20] is shown in Figure 7. Pulses of 1.2 ps duration at 800 nm were generated by a Ti:sapphire oscillator. These pulses were amplified at 1 kHz to a final energy of 3.0 mJ at 800 nm.[6] A custom-built mask in the pulse stretcher narrows the frequency bandwidth to produce pulses with a temporal fwhm of 1.2 ps. The output pulses are split into two roughly equal parts. One part is frequency doubled to 400 nm and used to pump two optical parametric amplifiers (OPAs, Light Conversion TOPAS 400/ps). One OPA is fixed at 532 nm for the Raman probe. The other OPA is tuned from 0.952 to 1.176 μm. In a potassium titanyl arsenate (KTA) crystal,[80] the second part of the 800 nm pulses plus the 0.952−1.176 μm

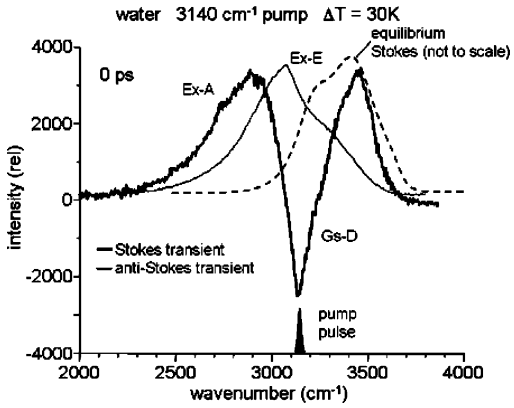

Figure 8. Raman spectrum of water (dashed curve) compared to Stokes and anti-Stokes transients obtained with 3140 cm^{-1} pump pulses, at a delay $t = 0$, with a final temperature increase $\Delta T = 30$ K. The anti-Stokes transient arises from excited-state emission (Ex-E) from ν_{OH} and a narrower blue-shifted band attributed to $\upsilon = 1$ states of H_2O^*. Excited states of H_2O^* are created by a two-step process: excitation of ν_{OH} followed by relaxation to H_2O^* $\upsilon = 0$ and subsequent IR pumping of H_2O^* to the $\upsilon = 1$ state.

pulses are combined to generate IR, tunable throughout the 2000−4000 cm^{-1} range. A typical IR pump pulse at 3310 cm^{-1} had a duration of 0.8 ps, a bandwidth of ~35 cm^{-1} and an approximately Gaussian spatial profile with ($1/e^2$) beam radius $r_0 = 150$ μm at the sample. The maximum IR pulse energy E_p was 43 μJ. The 10 μJ, 532 nm green probe pulses had a duration of 0.8 ps, a bandwidth of 25 cm^{-1}, and a beam diameter $r_0 =$ 120 μm. The smaller diameter Raman probe beam selectively interrogated water at the center of the pump beam.

The 532 nm Raman detection system was designed for simultaneous wide-aperture (f/1.4) collection in both Stokes and anti-Stokes regions (−3800 cm^{-1} to +3800 cm^{-1}) with a spectral resolution of 25 cm^{-1}. The emission from the sample originates from an ~100 μm diameter region, which is imaged at unit magnification onto the 100 μm spectrograph entrance slit with a pair of f/1.4 Nikon camera lenses. Between these lenses is a pair of holographic notch filters (Kaiser Optical) to remove elastically scattered light. An imaging spectrograph is used that consists of two f/1.4 Nikon camera lenses and a holographic volume grating (Kaiser Optical). The spectrograph images the spectral region 443−667 nm onto a detector array (Princeton Instruments) 1320 pixels in width. Each pixel is 22 μm wide, giving a dispersion of 5.8 cm^{-1}/pixel. The system resolution with a 100 μm slit is 25−30 cm^{-1}.

6. Results

In the results discussed here, unless otherwise noted the pump pulse intensities were adjusted to give $\Delta T = 30$ K. Figure 8 shows a typical pair of anti-Stokes and Stokes transients obtained at the time delay $t = 0$. A coherent artifact due to nonlinear light scattering (NLS) that appears near $t = 0$ has been subtracted away,[19,81,82] as described previously[20,83] and discussed below. The narrow-band pump pulse was centered at 3140 cm^{-1}, on the red edge of the water ν_{OH} transition (*dashed line* in Figure 8). The transient Stokes signal is bipolar. It has two peaks and one dip. The dip is caused by ground-state depletion. The red-shifted peak is caused by excited-state absorption ($|10\rangle \rightarrow |20\rangle$). The blue-shifted peak is caused by H_2O^* absorption ($\upsilon = 0 \rightarrow 1$). Keep in mind that the laser pulse duration of 0.8 ps is longer than the ~0.4 ps time to generate H_2O^* from ν_{OH}. The anti-Stokes transient is entirely due to excited-state emission ($|10\rangle \rightarrow |00\rangle$). The anti-Stokes spectrum has a double-peak structure.

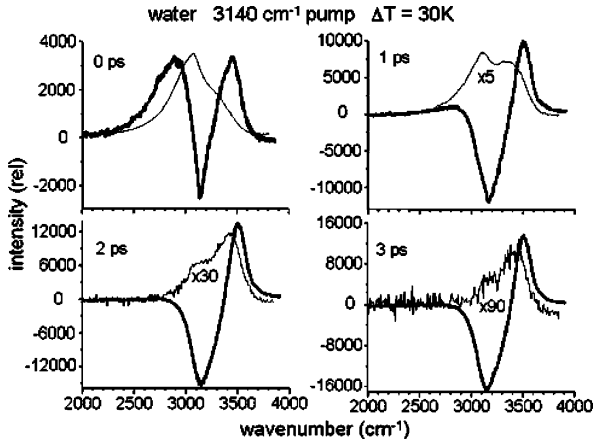

Figure 9. Stokes and anti-Stokes transients of water with red-edge pumping at 3140 cm^{-1} and $\Delta T = 30$ K at time delays up to 3 ps.

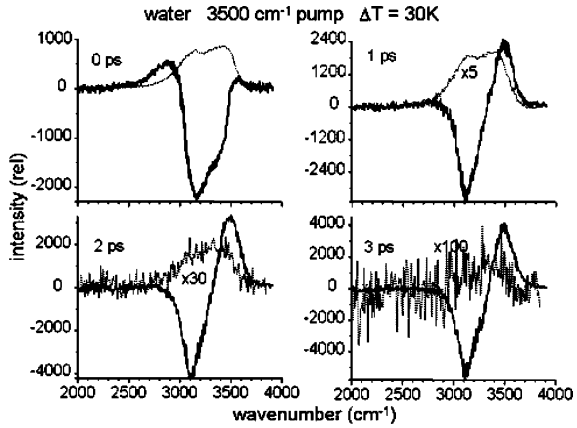

Figure 10. Stokes and anti-Stokes transients of water with blue-edge pumping at 3500 cm^{-1} and $\Delta T = 30$ K at time delays up to 3 ps.

The red-shifted peak is due to excited-state emission of water, and the blue-shifted peak to emission of H_2O^* in the $v = 1$ state.

Figures 9 and 10 show time-dependent Stokes and anti-Stokes transients obtained with either red-edge or blue-edge pumping. The NLS coherent artifact has been subtracted away. In the Stokes spectra, the excited-state absorption (on the red edge) decays within 1 ps. As time increases, the ground-state depletion (the dip at the pump wavenumber) broadens. The absorption on the blue edge grows in and broadens. At shorter times this feature is due to H_2O^*. At longer times, after ~1.5 ps this feature in the Stokes spectrum is caused by the weakened hydrogen bonding associated with the temperature increase ΔT. The Stokes spectrum in this case closely resembles what is expected for $\Delta T = 30$ K, shown in Figure 3b.

We now discuss the physical basis behind the features seen in Figures 8−10. The ground-state depletion feature in Figure 8 is broader than the spectral width of the IR pump pulse but narrower than the IR absorption or Stokes Raman spectrum. This is a hole burning effect that is a reflection of inhomogeneous broadening[18,19] of the ν_{OH} transition. Theorists using classical molecular dynamics simulations can simulate equilibrium fluctuations of the local hydrogen-bonding environment of a tagged water molecule.[25,26,28,30] As local structures fluctuate, the ν_{OH} transition frequency also fluctuates. When a molecule experiences stronger hydrogen bonding, the absorption is red-shifted; weaker hydrogen bonding leads to a blue shift. The frequency fluctuations can be characterized by a frequency time-correlation function[25] $\langle \Omega(0)\, \Omega(t) \rangle$, whose decay although clearly nonexponential in time[84] can be approximately described by a

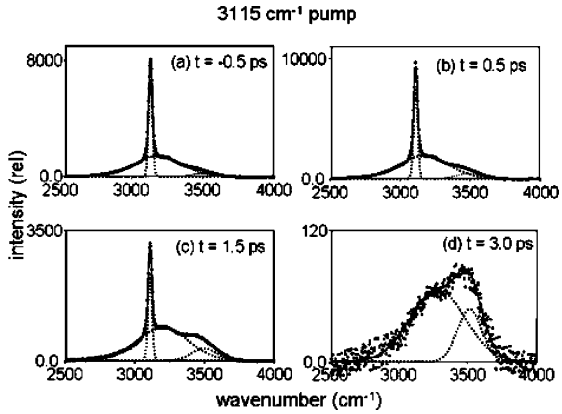

Figure 11. Transient anti-Stokes spectra in the ν_{OH} region of water with red-edge 3115 cm^{-1} pumping and $\Delta T = 30$ K. The spectra were fit using two Gaussian subbands plus a narrower Gaussian to represent the nonlinear light scattering (NLS) artifact. Reproduced from ref 20.

correlation time τ_c. When τ_c is a short time, molecules quickly lose memory of their original transition frequency, so narrow ground-state depletion features would not be observed. Because our IR pump pulse duration is 0.8 ps, the narrowed ground-state depletion feature in Figure 8 indicates that τ_c cannot be very much shorter than the 0.8 ps duration of the IR pump pulse, which is in good agreement with the cited classical simulations.[25,26,28,30]

Although the ground-state depletion is narrow, Figures 8−10 show that the excited-state emission is much broader. The excited-state emission has a two-peak structure. As discussed below, the blue-shifted peak is due to excited states of H_2O^*. The red-shifted peak has about the same width as the water IR absorption in the ν_{OH} region.[20] This indicates that in the ν_{OH} excited state $\tau_c \ll 0.8$ ps, in other words the frequency correlation function decays faster in the excited state. There are two reasons for this faster decay. First, the decay in the ground state observed via the ground-state depletion occurs via equilibrium fluctuations, but in the excited-state driven processes may also play a role. In the $v = 1$ state of ν_{OH}, hydrogen bonds (i.e., O···O distances) are expected to be a bit shorter than in $v = 0$, so upon excitation there is a driven reorganization of hydrogen bonding that both theory[25,26,28,30,33,72,85] and experiment[71,74,84,86] agree occurs on the 50−200 fs time scale. Second, in the excited-state vibrational excitations can quickly hop from one site to another[66] so as to rapidly experience different hydrogen-bonded environments without the need for oxygen or hydrogen atoms to move appreciably.

It is difficult to individually extract the excited-state absorption, ground-state depletion, H_2O^* absorption and thermalized absorption changes with high accuracy from the Stokes spectra, because they are broad and overlapping features, so henceforth we will concentrate on the anti-Stokes spectra that are entirely due to excited-state emission. The anti-Stokes spectra clearly show a two-component structure, with the component on the blue edge having the longer lifetime. This is true at all delay times and for all pump frequencies.[20] After 2 ps, only the longer-lived blue-shifted component of the excited-state spectrum remains. These longer-lived excited states are attributed to $v = 1$ of H_2O^*, which is produced by ν_{OH} created at the leading edge of the IR pump pulse and then subsequently driven into the $v = 1$ state by IR photons at the trailing edge of the pulse.[21,22] Figures 11 and 12 show how the ν_{OH} spectrum can be decomposed into two components (plus a NLS artifact), each having a Gaussian line shape.[20] This NLS artifact is spectrally much narrower than the water signal and it accurately tracks

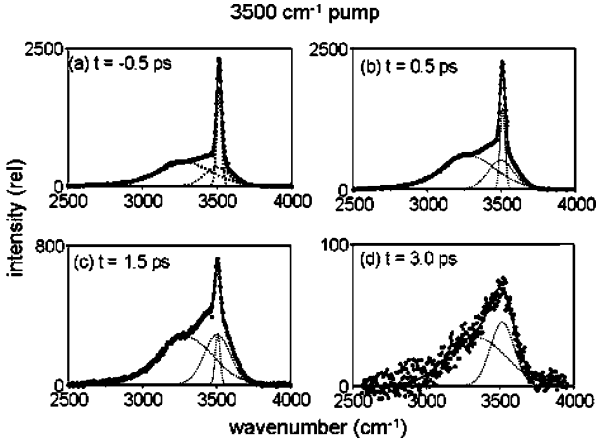

Figure 12. Transient anti-Stokes spectra in the ν_{OH} region of water with blue-edge 3500 cm^{-1} pumping and $\Delta T = 30$ K. The spectra were fit using two Gaussian subbands plus a narrower Gaussian to represent the nonlinear light scattering (NLS) artifact. Reproduced from ref 20.

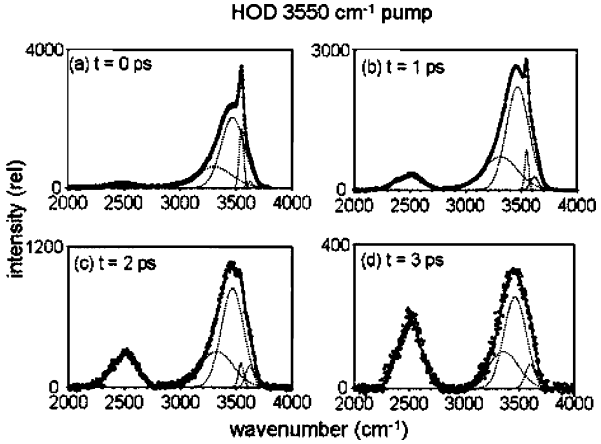

Figure 13. Transient anti-Stokes spectra in the ν_{OH} region of HOD/D_2O (10% HOD) with blue-edge 3550 cm^{-1} pumping and $\Delta T = 3$ K. A narrowed blue-shifted, longer-lived component is observed and attributed to HOD*. This observation shows that the generation of the metastable HOD* species depends on single-molecule behavior, not the value of ΔT. The broad band at ~2500 cm^{-1} is due to ν_{OD} excitations created by $\nu_{OH} \rightarrow \nu_{OD}$ relaxation. Reproduced from ref 20.

the IR−visible pulse cross-correlation, so we can easily subtract it from the spectra as shown in these figures. In earlier works the broader red-shifted and narrower blue-shifted components were termed ν_{OH}^{R} and ν_{OH}^{B}.[20,54−56,79,83] In light of the picture established by the works from all laboratories mentioned above, ν_{OH}^{R} is now attributed to water $\upsilon = 1$ excitations and ν_{OH}^{B} to H_2O*. Figures 11 and 12 show[20] that blue edge pumping produces a greater proportion of H_2O*, indicating that H_2O* has a blue-shifted absorption as well as a blue-shifted emission.

Figure 13 shows anti-Stokes spectra obtained using a solution of 10% HOD/D_2O.[20] In these experiments the excitation and pump conditions are the same as in the water experiments, but due to the reduced concentration of OH absorbers the temperature jump is reduced quite a bit $\Delta T \leq 8$ K.[20] Another significant difference is that, unlike the water measurements where the 0.2 ps ν_{OH} lifetime was much shorter than the 0.8 ps laser pulse duration, here the ν_{OH} lifetime of HOD is 0.9 ps. Figure 13 shows a new feature not seen in water, intermolecular vibrational energy transfer between isotopically distinct species. When ν_{OH} excitations decay, they generate ν_{OD} excitations of the D_2O solvent.[19]

As shown in Figure 13, the ν_{OH} region of HOD also can be described well with two Gaussian subbands (additional subbands

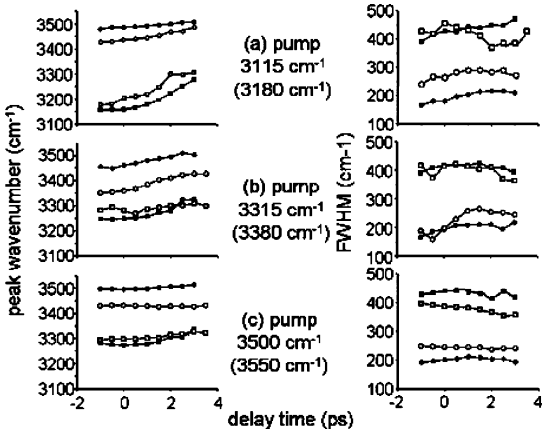

Figure 14. Time dependence of the peak locations and fwhm of the two Gaussian subbands seen in the anti-Stokes transients of water and HOD/D_2O: ν_{OH} (squares) and H_2O* (or HOD*, circles). Filled symbols represent water data; open symbols represent HOD data. The pump wavenumbers in parentheses correspond to the HOD/D_2O data. Reproduced from ref 20.

are needed to describe the ν_{OD} region).[20] To describe the blue-edge pumping measurements with high fidelity, it is also necessary to include a small subband on the blue edge, but this subband has the same time dependence as the dominant blue-shifted subband[20] associated with the nonthermalized species HOD*. The HOD data shows that the generation of HOD* is not associated with ΔT but is instead associated with single-molecule excitations. Additional evidence for HOD* can be found in recent work from the Fayer laboratory[11] who termed the species denoted here as HOD*, resulting from OD-stretch pumping, as a "transient photoproduct". The Fayer experiments involved much lower intensity energy bursts than in water experiments, because the OD-stretch energy is ~2500 cm^{-1} and the OD-stretch lifetime is 1.45 ps.[11] Fayer et al. reported that hydrogen bonds broke more slowly than in water (within ~800 fs compared to ~400 fs for water) and the HOD* decay to a thermalized ground state was also slower than in water (~1.5 ps compared to ~0.6 ps in water). It can be noted that the spectroscopic changes associated with this "transient photoproduct" are subtle and were not observed in a 2005 study from Bakker's laboratory.[87]

Figure 14 shows the peak frequencies and fwhm of the two excited-state $\upsilon = 1$ subbands of water and of HOD/D_2O created with red-edge pumping, mid-band pumping and blue-edge pumping. The HOD* band in HOD/D_2O is red-shifted by ~100 cm^{-1} and is ~50% broader than in water. As time progresses, the subbands typically undergo a blue shift, although the blue shift is minimal with the higher frequency pump pulses.[20] The fact that time and excitation frequency affects the H_2O* spectrum clearly indicates that the H_2O* species should not be viewed as a single state but rather as an inhomogeneous distribution of states.

Figure 15 provides information about the VR pathways of water and H_2O*. With red-edge pumping (Figure 15a) that produces little of the $\upsilon = 1$ excited state of H_2O*, excited states of δ_{H_2O} are observed. These excited bending vibrations are created by the $\nu_{OH} \rightarrow \delta_{H_2O}$ stretch-to-bend relaxation channel. However, with blue-edge pumping (Figure 15b) that creates much more H_2O*, there is little or no δ_{H_2O} observed.

Generally speaking, there are two ways to extract time-dependent information from data such as that in Figure 15. The more conventional method, which we term "single-wavenumber transients",[20] involves measuring the signal intensity versus time

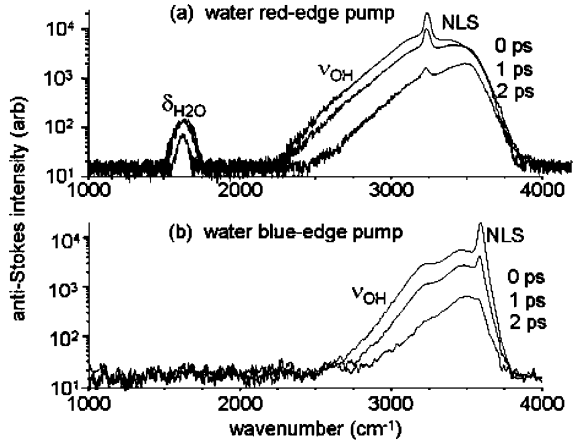

Figure 15. Transient anti-Stokes spectra of water with red-edge pumping at 3200 cm^{-1} and blue-edge pumping at 3600 cm^{-1} and ΔT = 30 K. The narrower peak at the pump wavenumber is an artifact due to nonlinear light scattering (NLS). δ_{H_2O} is observed with red-edge pumping but not with blue-edge pumping. Reproduced from ref 20.

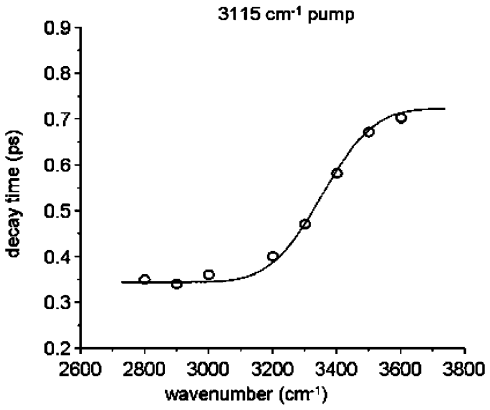

Figure 16. Anti-Stokes data for water with 3115 cm^{-1} red-edge pumping, analyzed by the single-wavenumber transient method.[20] An effective exponential decay time constant is extracted at each probe wavenumber interval (10 cm^{-1}) by fitting the time-dependent intensities with the convolution of the laser apparatus time response obtained from nonlinear light scattering along with a single-exponential function. The time constant on the red edge represents ν_{OH} decay and the time constant on the blue edge reflects H_2O^* decay. Adapted from ref 20.

at a fixed wavenumber. Pump−probe experiments using narrow-band probe pulses automatically measure these single-wavenumber transients. As an example, we extracted single-wavenumber transients from data obtained with red-edge 3115 cm^{-1} pumping. An exponential decay was convolved with the apparatus response determined using NLS and then the decay constant was varied to obtain the best fit to the data. As shown in Figure 16, this decay time constant ranged from 0.35 ps on the red edge to 0.7 ps on the blue edge. The single-wavenumber approach for water has been criticized by more than one author because the single-wavenumber decay constant can reflect both population dynamics and spectral evolution.[62,63,71,75] Spectral evolution away from the probed wavenumber increases the decay rate, and spectral evolution toward the probed wavenumber decreases the decay rate regardless of the population dynamics. An alternative procedure developed by Laubereau's group[61] involves plotting the time-dependent amplitudes of Gaussian subbands that might be frequency-shifting as the amplitude decays, which is clearly the case here as shown in Figure 14. The results of this Gaussian subband analysis are shown in Figure 17. The NLS signal represents the apparatus time response function. With red-edge pumping (Figure 17a),

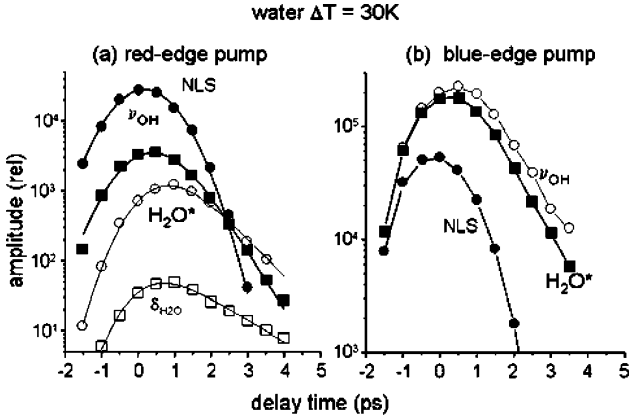

Figure 17. Time dependence of the subband amplitudes in water. NLS denotes the nonlinear light-scattering coherence artifact that gives the apparatus time response. (a) With red-edge pumping the ν_{OH} subband builds up instantaneously and the H_2O^* subband and the δ_{H_2O} bending excitation have a delayed buildup. (b) With blue-edge pumping both subbands build up instantaneously; at longer delay times both subbands decay with the H_2O^* lifetime. Adapted from ref 20.

ν_{OH} builds up instantaneously (as determined by the NLS signal) and then decays with a time constant T_1 = 0.55 (±0.05) ps. The H_2O^* has a delayed buildup.[56] The H_2O^* lifetime is T_1 = 0.75 (±0.08) ps. The δ_{H_2O} bending vibration buildup mirrors the ν_{OH} decay, and the δ_{H_2O} lifetime is T_1 = 1.4 ps. With blue-edge pumping both ν_{OH} and H_2O^* subbands appear to build up instantaneously, and both decay with a T_1 = 0.75 ps lifetime.

7. Discussion

7.1. Brief Summary of Experimental Results. Let us begin by summarizing our most significant results:

1. We see two kinds of water. This is most evident in the anti-Stokes spectra that arise from $v = 1$ excitations (see Figures 11−13). There is a red-shifted subband associated with ν_{OH} of water and a blue-shifted subband associated with H_2O^*.

2. The H_2O^* species has a blue-shifted and narrowed emission spectrum compared to ν_{OH}. The H_2O^* emission can be fitted using a Gaussian line shape peaked at ∼3500 cm^{-1} with a fwhm of ∼200 cm^{-1}.

3. The H_2O^* species has a longer excited-state lifetime than ν_{OH}, and its VR occurs by a characteristically different mechanism that appears to produce much less δ_{H_2O} excitation.

7.2. Nature of H_2O^*. We can understand a great deal about H_2O^* by looking at equilibrium water spectra as a function of temperature and pressure. Even a brief inspection of water Raman spectra under extreme conditions[88,89] makes a very strong case that H_2O^* *looks a great deal like supercritical water*. For instance, the Raman spectrum[88] at P = 40 MPa, T = 300 °C quite closely resembles our H_2O^* spectra, with a peak at 3550 cm^{-1} and a fwhm of 200 cm^{-1}.

Now some caveats are in order, because the H_2O^* state we see is metastable and cannot be replicated in an equilibrium experiment. The local conditions due to the energy burst from the ν_{OH} relaxation approximate a state of high pressure and high temperature, but the density is fixed by inertial confinement at 1000 kg/m^3.

A 1998 study on Raman spectroscopy of supercritical water[88] concluded that the strength of hydrogen bonding does not vary much with temperature up to 500 °C at constant density. In other words, the blue-shifting and narrowing of the water equilibrium ν_{OH} spectrum with increasing temperature is attributed mainly to a density decrease. Very close to the critical point (P_c = 22.1 MPa, T_c = 374 °C, ρ_c = 322 kg/m^3), the ν_{OH}

spectrum is peaked at 3620 cm^{-1} with a fwhm of only 60 cm^{-1}. Conditions where a spectrum very much like H_2O^* is observed[88,89] ($P = 40$ MPa, $T = 300$ °C) correspond to a greater density $\rho \approx 600$ kg/m^3. So we think it is fair to conclude that H_2O^* is characterized by a local environment with the strength of hydrogen bonding similar to that of water at a density of 0.6 g/cm^3.

As discussed above, the spectrum we associate with H_2O^* clearly represents an inhomogeneous distribution of structures, but we have to wonder why all our results seem to be consistent with mainly two, rather than a multitude of water species.[20] The most satisfying resolution of this question is to think of H_2O^* as being water with a single broken donor hydrogen bond, as suggested by the Fayer group,[11] along with a broad distribution of other structural parameters. For us it is difficult to understand why there would be a sharp distinction between "intact" and "broken" hydrogen bonds in the dense liquid state. However, it should be noted that models that posit a sharp cut off for hydrogen bonding, when used to calculate the spectrum of water with a single broken donor hydrogen bond,[28,30] do output results that closely resemble our anti-Stokes spectra.[20]

7.3. Interpretation of Time Constants Seen in IR−Raman Measurements. In our anti-Stokes spectra, the ν_{OH} and H_2O^* species have broad overlapping spectra. But at longer delay times on the blue edge of the spectrum, H_2O^* is totally dominant, so we regard our lifetime measurements of H_2O^* as reliable. The buildup of H_2O^* occurs with an apparent 0.55 ps time constant,[20] which is associated with the loss of vibrational energy, both stretching and bending, from vibrationally excited water. Measurements by other groups using shorter pulses give a more accurate value for this time constant of 0.44 ps.[7] The decay of vibrationally excited $\upsilon = 1$ H_2O^* occurs with a lifetime of 0.75 ps.[20] As discussed below, it is interesting that this time constant is very close to the thermalization time constant (ranging from 0.6 to 0.8 ps) seen in numerous IR experiments,[7,12,13,15,16] which represents the decay of ground-state H_2O^* back to ordinary water.

For ν_{OH} relaxation, it is unlikely that we can get an accurate value with our longer-duration pulses. Still it seems that the most reliable values should be obtained with pumping and probing at the red edge. In this case Figure 16 gives a decay time constant of 0.35 ps. This time constant appears to correspond to the 0.2 ps lifetime seen in measurements using shorter duration pulses.[7,12,13,15,16,18]

There are some features seen in our kinetics that are difficult to understand. These are the time constants for ν_{OH} decay in Figure 17a,b and for δ_{H_2O} decay in Figure 17a. In Figure 17a, the ν_{OH} decay is best fitted using a 0.55 ps time constant, and δ_{H_2O} evidences an unreasonably long tail out to several picoseconds, which is inconsistent with its known 0.2 ps lifetime. In Figure 17b where blue-edge pumping is used, the apparent ν_{OH} lifetime asymptotically approaches the 0.75 ps H_2O^* lifetime.

7.4. Mechanism of H_2O^* Relaxation. The relaxation of H_2O^* into water has previously been described as a "thermalization" process.[15,16] In light of our discussion of the hydrogen-bond disruption associated with H_2O^*, we should refine this interpretation to include hydrogen-bond re-formation.[56] As the burst of energy created by ν_{OH} relaxation dissipates, the disrupted hydrogen-bond network will re-form into an equilibrium state consistent with a new temperature elevated by ΔT. We could view this as a two-step process, energy dissipation followed by hydrogen-bond re-formation, leading to the measured lifetime of 0.8 ps. Molecular simulations show that hydrogen-bond re-formation occurs in about 1 ps,[1,90−93] which is suggestive that re-formation, rather than energy dissipation is the rate-limiting step in H_2O^* relaxation.

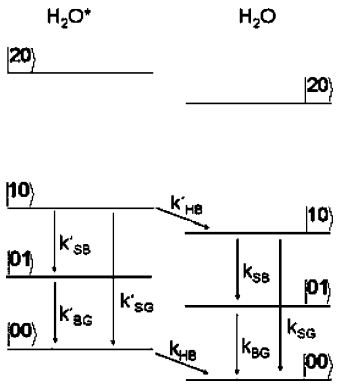

Figure 18. Level diagram for the relaxation of H_2O^* in the ground and vibrationally excited state. The notation $|nn'\rangle$ means n quanta of stretch and n' quanta of bend. In its vibrational ground state, H_2O^* relaxes to water by re-forming the disrupted hydrogen-bond network with rate constant k_{HB}. Vibrationally excited H_2O^* could relax to create vibrationally excited water, by hydrogen-bond re-formation with rate constant k'_{HB}, or by stretch-to-bend or stretch-to-ground-state relaxation with rate constants k'_{SB} or k'_{SG}.

The relaxation of vibrationally excited H_2O^* is illustrated in Figure 18. The relaxation could occur either by hydrogen-bond re-formation, to create vibrationally excited H_2O (i.e., ν_{OH}) with rate constant k'_{HB}, or by stretch-to-bend or stretch-to-ground-state relaxation with rate constants k'_{SB} or k'_{SG}. We believe we should rule out the possibility that $\upsilon = 1$ H_2O^* relaxes into the vibrational ground state of H_2O; this would involve making new hydrogen bonds while simultaneously releasing a large packet of energy.

The major features in our data could be explained if H_2O^* $\upsilon = 1$ relaxes by either one of two mechanisms, stretch-to-ground-state or hydrogen-bond re-formation. However, we tend to favor the latter explanation for two reasons. First, the fact that the measured lifetimes of ground-state H_2O^* (0.8 ps) and vibrationally excited H_2O^* (0.75 ps) are identical is suggestive that both relax by the hydrogen-bond re-formation mechanism. In other words in Figure 18, $k'_{HB} \approx k_{HB}$. Second, there are two minor features of our data, the long tail in the δ_{H_2O} decay in Figure 17a and the convergence of the ν_{OH} and H_2O^* decays in Figure 17b, which seem more consistent with hydrogen-bond re-formation. In this view the low-amplitude long-time tails of ν_{OH} and δ_{H_2O} are generated by the process

$$H_2O^*(\upsilon{=}1) \xrightarrow[k'_{HB}]{0.8\ \text{ps}} \nu_{OH} \xrightarrow[k_{SB}]{0.2\ \text{ps}} \delta_{H_2O} \xrightarrow[k_{BG}]{0.2\ \text{ps}} \text{ground state}$$

With the pulse durations used in our experiments, the ν_{OH} and δ_{H_2O} species will be low-concentration short-lived intermediates in the steady state and will appear to contribute very little to our observed spectra.

8. Summary and Conclusion

The 1982 work by Vodopyanov and co-workers[68] was remarkably insightful. They deduced that vibrational absorption of ν_{OH} in water, using intense 100 ps IR pulses, was strongly affected by weakened hydrogen bonding resulting from multiple successive excitations combined with adiabatic isochoric heating occurring during the pump pulse. Using a measured energy density of 1 kJ/cm^3, they deduced a temperature rise of 235 K at the end of the pulse which, assuming eq 2 holds, corresponds to a pressure of 420 MPa. They then displayed temperature-

dependent IR spectra from 20 to 500 °C of HOD/D_2O, obtained in studies of supercritical water at 25 MPa, showing a strong blue shift and narrowing effect similar to what we see for H_2O^*. However, because the Vodopyanov experiments were not time-resolved, the effects that were observed could not be attributed to metastable states such as H_2O^*, but rather to laser-generated thermalized supercritical water.

Ultrafast IR pump−probe experiments have done a good job of measuring time constants associated with H_2O^* formation and decay, but so far IR probe methods have not done a good job obtaining reliable spectra of H_2O^* or its cousin HOD*. We believe this is a consequence of the nature of these probe methods. At longer delay times when vibrationally excited water has disappeared and only the longer-lived H_2O^* is present, the IR spectrum is dominated by the derivative spectra (e.g., Figure 3) associated with ΔT, so reliably extracting the smaller H_2O^* contribution is difficult.[11] We can suggest an intriguing method to study H_2O^*, a pump−pump−probe method where a first pump pulse is used to generate H_2O^* from ν_{OH} relaxation. At a time of about 500 fs when all ν_{OH} and δ_{H_2O} excitations have decayed, a subsequent pump pulse would prepare $v = 1$ states of H_2O^*, which could then be probed by the usual methods.

The ability to more accurately characterize H_2O^* in our IR−Raman experiments stems from two factors, the longer-duration pump pulses that in effect function like the double pump pulses mentioned above, to create a sizable population of $v = 1$ H_2O^*, and the unique ability of anti-Stokes Raman to selectively probe excited states only. In our experiments we are able to extract a clean, unambiguous spectrum of H_2O^*,[20] showing a peak at ~3500 cm^{-1} and a fwhm of 200 cm^{-1}. Comparison with equilibrium spectra then suggests that H_2O^* looks a great deal like supercritical water at ~300 °C (~600 K), which is consistent with our admittedly simplistic estimates of the effective temperatures obtained by redistributing the energy of a single ν_{OH} excitation on a single water molecule ($T = 1100$ K), two molecules ($T = 700$ K), three molecules ($T = 570$ K), etc. The disappearance of H_2O^* in both the $v = 0$ and $v = 1$ states seems to occur by the same mechanism, re-formation of the disrupted hydrogen-bonding network.

What are the implications of this unique metastable state of water created by ν_{OH} excitation? The first is simply a sense of wonder that vibrational energy in water is weirder and more interesting than we had imagined. It is not that ν_{OH} excitation causes hydrogen bonds to break directly, via vibrational predissociation as suggested by theorists and observed frequently in gas-phase clusters, but rather the disruption results from an indirect process: the energy burst created by the extremely short-lived vibrational excitations in water.

Another intriguing question is, what is happening in our IR spectrometers?[94] Certainly with a low IR flux and a liquid water sample, H_2O^* is simply a fleeting and inconsequential transient, but this might not be the case for the ubiquitous confined water found in reverse micelles, in hydrophobic media, in porous materials and on the surfaces of biological macromolecules.[95] Perhaps the hydrogen-bond disruption that accompanies ν_{OH} excitation in such systems could be long-lived and consequential.

Arguably the most important implication of H_2O^* involves the implication for theoretical studies of VR in aqueous media. Theoretical calculations of VR in polyatomic liquids have proven to be a difficult challenge because, when $h\nu \gg kT$, the quantum mechanical nature of the excitations cannot be disregarded. The most successful theoretical works[34,35,38 ,39,96] utilize the Landau−Teller approximation. A vibrational excitation in a liquid experiences rapidly fluctuating forces from the bath, which can induce transitions between the excited and ground states. These forces are characterized by a force−force correlation function averaged over all bath degrees of freedom Q, $\langle \hat{F}(t)\ \hat{F}(0)\rangle_Q$. In the Landau−Teller method, the inverse vibrational lifetime $(T_1)^{-1}$ is proportional to the Fourier transform of this force−force correlation function at the oscillator frequency. It is exceedingly difficult to calculate the full quantum mechanical correlation function, so ordinarily a classical molecular dynamics (MD) simulation is used to calculate a classical analog $\langle F(t)\, F(0)\rangle$, yielding an expression for the vibrational lifetime,

$$(T_1)^{-1} = \frac{Q_c}{2\mu h\nu} \int_{-\infty}^{+\infty} \mathrm{d}t\ \mathrm{e}^{2\pi i\nu t} \langle F(t)\, F(0)\rangle_Q \qquad (3)$$

where Q_c is a quantum correction factor[97,98] and μ is the reduced mass.

In deriving eq 3, an important assumption of linear response (weak coupling) is made. It is assumed that excitation or VR of the oscillator does not strongly perturb the bath, and this assumption is what makes it possible to calculate T_1 using an equilibrium MD simulation to determine the relaxation of oscillators driven away from equilibrium. Although this assumption is probably excellent for many molecular liquids, in water the fast burst of energy and the fragility of the local hydrogen-bonding network result in a large disruption of the bath, which casts doubt on this central assumption. It may well be that Landau−Teller is adequate to calculate the lifetimes of ν_{OH} and δ_{H_2O} observed in pump−probe experiments, but it seems doubtful that equilibrium methods would be useful to understand subsequent events such as VR of the daughter δ_{H_2O} excitations created by a ν_{OH} parent, the behavior of H_2O^* and so on. Nonequilibrium simulations such as those used by Dong and Wheeler[43] to investigate water VR or by Kabadi and Rice[99] to investigate VR of nitromethane[100] might be needed.

Acknowledgment. This material is based on work supported by the National Science Foundation under award DMR-05 04038. Additional support was provided by the U.S. Air Force Office of Scientific Research under award number F49620-03-1-0032. We gratefully acknowledge many helpful conversations with Prof. H. Bakker, and we thank Prof. T. Elsaesser for sharing his recent results prior to publication.

References and Notes

(1) Rahman, A.; Stillinger, F. H. *J. Chem. Phys.* **1971**, *55*, 3336.
(2) Ball, P. *Life's Matrix: A Biography of Water*; University of California: Berkeley, 2001.
(3) Nibbering, E. T. J.; Elsaesser, T. *Chem. Rev.* **2004**, *104*, 1887.
(4) Staib, A.; Hynes, J. T. *Chem. Phys. Lett.* **1993**, *204*, 197.
(5) Steinbach, C.; Andersson, P.; Kazimirski, J. K.; Buck, U.; Buch, V.; Beu, T. A. *J. Phys. Chem. A* **2004**, *108*, 6165.
(6) Wang, Z.; Pang, Y.; Dlott, D. D. *Chem. Phys. Lett.* **2004**, *397*, 40.
(7) Elsaesser, T.; Ashihara, S.; Huse, N.; Espagne, A.; Nibbering, E. *J. Phys. Chem. A* **2007**, *111*, 743.
(8) Asbury, J. B.; Steinel, T.; Fayer, M. D. *J. Phys. Chem. B* **2004**, *108*, 6544.
(9) Asbury, J. B.; Steinel, T.; Stromberg, C.; Gaffney, K. J.; Piletic, I. R.; Fayer, M. D. *J. Chem. Phys.* **2003**, *119*, 12981.
(10) Gaffney, J. J.; Piletic, I. R.; Fayer, M. D. *J. Phys. Chem. A* **2002**, *106*, 9428.
(11) Steinel, T.; Asbury, J. B.; Zheng, J. R.; Fayer, M. D. *J. Phys. Chem. A* **2004**, *108*, 10957.
(12) Huse, N.; Ashihara, S.; Nibbering, E. T. J.; Elsaesser, T. *Chem. Phys. Lett.* **2005**, *404*, 389.
(13) Lindner, J.; Vohringer, P.; Pshenichnikov, M. S.; Cringus, D.; Wiersma, D. A.; Mostovoy, M. *Chem. Phys. Lett.* **2006**, *421*, 329.
(14) Ashihara, S.; Huse, N.; Espagne, A.; Nibbering, E. T. J.; Elsaesser, T. *Chem. Phys. Lett.* **2006**, *424*, 66.
(15) Lock, A. J.; Bakker, H. J. *J. Chem. Phys.* **2002**, *117*, 1708.

(16) Lock, A. J.; Woutersen, S.; Bakker, H. J. *J. Phys. Chem. A* **2001**, *105*, 1238.
(17) Wang, Z.; Pang, Y.; Dlott, D. D. *J. Phys. Chem. B* **2006**, *110*, 201150.
(18) Cowan, M. L.; Bruner, B. D.; Huse, N.; Dwyer, J. R.; Chugh, B.; Nibbering, E. T. J.; Elsaesser, T.; Miller, R. J. D. *Nature* **2005**, *434*, 199.
(19) Deàk, J. C.; Iwaki, L. K.; Dlott, D. D. *J. Phys. Chem.* **2000**, *104*, 4866.
(20) Wang, Z.; Pakoulev, A.; Pang, Y.; Dlott, D. D. *J. Phys. Chem.* **2004**, *108*, 9054.
(21) Bakker, H. J.; Lock, A. J.; Madsen, D. *Chem. Phys. Lett.* **2004**, *385*, 329.
(22) Bakker, H. J.; Lock, A. J.; Madsen, D. *Chem. Phys. Lett.* **2004**, *384*, 236.
(23) Herzberg, G. *Molecular Spectra and Molecular Structure II. Infrared and Raman Spectra of Polyatomic Molecules*; Van Nostrand Reinhold: New York, 1945.
(24) Ahlborn, H.; Ji, X.; Space, B.; Moore, P. B. *J. Chem. Phys.* **1999**, *111*, 10622.
(25) Lawrence, C. P.; Skinner, J. L. *J. Chem. Phys.* **2003**, *118*, 264.
(26) Møller, K. B.; Rey, R.; Hynes, J. T. *J. Phys. Chem. A* **2004**, *108*, 1275.
(27) Diraison, M.; Leicknam, J.-C.; Tarjus, G.; Bratos, S. *Phys. Rev. E* **1994**, *50*.
(28) Rey, R.; Møller, K. B.; Hynes, J. T. *J. Phys. Chem. A* **2002**, *106*, 11993.
(29) Lawrence, C. P.; Skinner, J. L. *J. Chem. Phys.* **2002**, *117*, 8847.
(30) Lawrence, C. P.; Skinner, J. L. *Chem. Phys. Lett.* **2003**, *369*, 472.
(31) Walrafen, G. E.; Blatz, L. A. *J. Chem. Phys.* **1973**, *59*, 2646.
(32) Walrafen, G. E.; Hokmabadi, M. S.; Yang, W. H. *J. Phys. Chem.* **1988**, *92*, 2433.
(33) Bratos, S.; Leicknam, J.-C. *J. Chem. Phys.* **1994**, *101*, 4536.
(34) Lawrence, C. P.; Skinner, J. L. *J. Chem. Phys.* **2002**, *117*, 5827.
(35) Lawrence, C. P.; Skinner, J. L. *J. Chem. Phys.* **2003**, *119*, 1623.
(36) Lawrence, C. P.; Skinner, J. L. *Chem. Phys. Lett.* **2003**, *372*, 842.
(37) Lawrence, C. P.; Skinner, J. L. *J. Chem. Phys.* **2003**, *119*, 3840.
(38) Rey, R.; Møller, K. B.; Hynes, J. T. *Chem. Rev.* **2004**, *104*, 1915.
(39) Rey, R.; Hynes, J. T. *J. Chem. Phys.* **1996**, *104*, 2356.
(40) Steinel, T.; Asbury, J. B.; Corcelli, S. A.; Lawrence, C. P.; Skinner, J. L.; Fayer, M. D. *Chem. Phys. Lett.* **2004**, *386*, 295.
(41) Corcelli, S. A.; Lawrence, C. P.; Skinner, J. L. *J. Chem. Phys.* **2004**, *120*, 8107.
(42) Asbury, J. B.; Steinel, T.; Kwak, K.; Corcelli, S. A.; Lawrence, C. P.; Skinner, J. L.; Fayer, M. D. *J. Chem. Phys.* **2004**, *121*, 12431.
(43) Dong, H.; Wheeler, R. A. *Chem. Phys. Lett.* **2005**, *413*, 176.
(44) Hadži, D.; Bratos, S. *The Hydrogen Bond*; Elsevier: Amsterdam, 1976.
(45) Jorgensen, W. L.; Madura, J. D. *Mol. Phys.* **1985**, *56*, 1381.
(46) Bertie, J. E.; Lan, Z. *Appl. Spectrosc.* **1996**, *50*, 1047.
(47) Amir, W.; Gallot, G.; Hache, F. *J. Chem. Phys.* **2004**, *121*, 7908.
(48) Hare, D. E.; Franken, J.; Dlott, D. D. *J. Appl. Phys.* **1995**, *77*, 5950.
(49) Wang, Z.; Pakoulev, A.; Pang, Y.; Dlott, D. D. Three-dimensional spectroscopy of vibrational energy relaxation in liquids. In *Femtochemistry and Femtobiology. Ultrafast Events in Molecular Science*; Martin, M. M., Hynes, J. T., Eds.; Elsevier: Amsterdam, 2004; pp 169.
(50) Seifert, G.; Patzlaff, T.; Graener, H. *J. Chem. Phys.* **2004**, *120*, 8866.
(51) Seifert, G.; Patzlaff, T.; Graener, H. *J. Chem. Phys.* **2006**, *125*, 154506.
(52) Stillinger, F. H.; Weber, T. A. *Phys. Rev. A* **1982**, *25*, 978.
(53) Deàk, J. C.; Iwaki, L. K.; Rhea, S. T.; Dlott, D. D. *J. Raman Spectrosc.* **2000**, *31*, 263.
(54) Pakoulev, A.; Wang, Z.; Dlott, D. D. *Chem. Phys. Lett.* **2003**, *371*, 594.
(55) Pakoulev, A.; Wang, Z.; Pang, Y.; Dlott, D. D. *Chem. Phys. Lett.* **2003**, *380*, 404.
(56) Wang, Z.; Pakoulev, A.; Pang, Y.; Dlott, D. D. *Chem. Phys. Lett.* **2003**, *378*, 281.
(57) Wang, Z.; Pang, Y.; Dlott, D. D. *J. Chem. Phys.* **2004**, *120*, 8345.
(58) Laubereau, A.; Kaiser, W. *Rev. Mod. Phys.* **1978**, *50*, 607.
(59) Seilmeier, A.; Kaiser, W. Ultrashort intramolecular and intermolecular vibrational energy transfer of polyatomic molecules in liquids. In *Ultrashort Laser Pulses and Applications*; Kaiser, W., Ed.; Springer-Verlag: Berlin, 1988; Vol. 60, pp 279.
(60) Fayer, M. D. *Ultrafast infrared and Raman spectroscopy*; Marcel Dekker, Inc.: New York, 2001.
(61) Graener, H.; Seifert, G.; Laubereau, A. *Phys. Rev. Lett.* **1991**, *66*, 2092.
(62) Laenen, R.; Rauscher, C.; Laubereau, A. *J. Phys. Chem. B* **1998**, *102*, 9304.
(63) Laenen, R.; Rauscher, C.; Laubereau, A. *Phys. Rev. Lett.* **1998**, *80*, 2622.
(64) Woutersen, S.; Emmerichs, U.; Bakker, H. J. *Science* **1997**, *278*, 658.
(65) Nienhuys, H.-K.; Woutersen, S.; van Santen, R. A.; Bakker, H. J. *J. Chem. Phys.* **1999**, *111*, 1494.
(66) Woutersen, S.; Bakker, H. J. *Nature* **1999**, *402*, 507.
(67) Doktor, A. M.; Woutersen, S.; Bakker, H. J. *Proc. Natl. Acad. Sci. U.S.A.* **2006**, *103*, 15355.
(68) Vodopyanov, K. L. *J. Chem. Phys.* **1991**, *94*, 5389.
(69) Siegman, A. E. *Lasers*; University Science Books: Sausalito, CA, 1986.
(70) Woutersen, S.; Emmerichs, U.; Nienhuys, H.-K.; Bakker, H. J. *Phys. Rev. Lett.* **1998**, *81*, 1106.
(71) Woutersen, S.; Bakker, H. J. *Phys. Rev. Lett.* **1999**, *83*, 2077.
(72) Bratos, S.; Leicknam, J.-C. *J. Chem. Phys.* **1995**, *103*.
(73) Gale, G. M.; Gallot, G.; Hache, F.; Lascoux, N.; Bratos, S.; Leicknam, J.-C. *Phys. Rev. Lett.* **1999**, *82*, 1068.
(74) Bratos, S.; Gale, G. M.; Gallot, G.; Hache, F.; N. Lascoux, N.; Leicknam, J.-C. *Phys. Rev. E* **2000**, *61*, 5211.
(75) Gale, G. M.; Gallot, G.; Lascoux, N. *Chem. Phys. Lett.* **1999**, *311*, 123.
(76) Dlott, D. D. *Chem. Phys.* **2001**, *266*, 149.
(77) Deàk, J. C.; Pang, Y.; Sechler, T. D.; Wang, Z.; Dlott, D. D. *Science* **2004**, *306*, 473.
(78) Cringus, D.; Lindner, J.; Milder, M. T. W.; Pshenichnikov, M. S.; Vöhringer, P.; Wiersma, D. A. *Chem. Phys. Lett.* **2005**, *408*.
(79) Pakoulev, A.; Wang, Z.; Pang, Y.; Dlott, D. D. *Chem. Phys. Lett.* **2004**, *385*, 332.
(80) Deàk, J. C.; Iwaki, L. K.; Dlott, D. D. *Opt. Lett.* **1997**, *22*, 1796.
(81) Kauranen, M.; Persoons, P. *J. Chem. Phys.* **1996**, *104*, 3445.
(82) Terhune, R. W.; Maker, P. D.; Savage, C. M. *Phys. Rev. Lett.* **1965**, *14*, 681.
(83) Iwaki, L. K.; Dlott, D. D. *J. Phys. Chem. A* **2000**, *104*, 9101.
(84) Fecko, C. J.; Eaves, J. D.; Loparo, J. J.; Tokmakoff, A.; Geissler, P. L. *Science* **2003**, *301*, 1698.
(85) Diraison, M.; Guissani, Y.; Leicknam, J.-C.; Bratos, S. *Chem. Phys. Lett.* **1996**, *258*, 348.
(86) Gallot, G.; Lascoux, N.; Gale, G. M.; Leicknam, J.-C.; Bratos, S.; Pommeret, S. *Chem. Phys. Lett.* **2001**, *341*, 535.
(87) Rezus, Y. L. A.; Bakker, H. J. *J. Chem. Phys.* **2005**, *123*, 114502.
(88) Ikushima, Y.; Hatakeda, K.; Saito, N. *J. Chem. Phys.* **1998**, *198*, 5855.
(89) Lin, J.-F.; Militzer, B.; Struzhkin, V. V.; Gregoryanz, E.; Hemley, R. J.; Mao, H. *J. Chem. Phys.* **2004**, *121*, 8423.
(90) Luzar, A. *J. Chem. Phys.* **2000**, *113*, 10663.
(91) Luzar, A.; Chandler, D. *Nature* **1996**, *379*, 55.
(92) Stern, H. A.; Berne, B. J. *J. Chem. Phys.* **2001**, *115*, 7622.
(93) Xu, H.; Stern, H. A.; Berne, B. J. *J. Phys. Chem. B* **2002**, *106*, 2054.
(94) Piletic, I. R.; Moilanen, D. E.; Levinger, N. E.; Fayer, M. D. *J. Am. Chem. Soc.* **2006**, *128*, 10366.
(95) *Biomolecules in Organic Solvents*; Gómez-Puyou, A., Ed.; CRC Press: Boca Raton, FL, 1992.
(96) Bakker, H. J. *J. Chem. Phys.* **2004**, *121*, 10088.
(97) Bader, J. S.; Berne, B. J. *J. Chem. Phys.* **1994**, *100*, 8359.
(98) Skinner, J. L.; Park, K. *J. Phys. Chem. B* **2001**, *105*, 6716.
(99) Kabadi, V. N.; Rice, B. M. *J. Phys. Chem. A* **2004**, *108*, 532.
(100) Deàk, J. C.; Iwaki, L. K.; Dlott, D. D. *J. Phys. Chem. A* **1999**, *103*, 971.